



Mechanism of negative surface charge formation on biochar and its effect on the fixation of soil Cd



Zhongxin Tan*, Shengnan Yuan, Mengfan Hong, Limei Zhang, Qiaoyun Huang

Hubei Key Laboratory of Soil Environment and Pollution Remediation, College of Resources and Environment, Huazhong Agricultural University, No. 1 Lion Hill Street, Hongshan District, Wuhan, 430070, PR China

ARTICLE INFO

Editor: Deyi Hou

Keywords:

Biochar

Soil Cd fixation

Electronegativity

Oxygen-containing functional groups

ABSTRACT

The studies of the mechanism of Cd fixation by biochar have mainly focused on the pore size, pH, and oxygen-containing functional groups, and few researches have paid close attention to the effect of the negative charge in biochar surface. In this paper, biochar was produced in the CO₂ atmosphere at different pyrolysis temperatures, and the influence of the pyrolysis temperature on biochar surface charge were explored. The cause of the negative charge on the biochar surface has been analysed, and the optimal preparing temperature for the biochar with the best effect of cadmium immobilization from soil has been found. The results show that with the increasing temperature from 300 to 700 °C, the negative surface charge on biochar surface gradually decreases, while the fixed amount of Cd increases. The factors affecting the surface charge of biochar are ash content, pH, oxygen-containing functional groups, polar groups, and hydrogen bonds. Among them, the pH, oxygen-containing functional groups and polar groups have positive effects on the surface negative charge, whereas the hydrogen bond has a negative effect. The determinant of surface charge is the hydroxyl group, the content of hydroxyl group decreases as increasing temperature, resulting in a decrease in surface negative charge.

1. Introduction

Heavy metal contamination in the soil is becoming increasingly problematic (Toth et al., 2016), among which, Cd pollution is particularly serious. According to the National Soil Pollution Survey Bulletin conducted by the State Council on April 17, 2014 can be seen that the pollution type is mainly inorganic. The over-standard rates of four inorganic pollutants such as cadmium, mercury, arsenic and lead were 7.0%, 1.6, 2.7% and 1.5%, respectively, and the cadmium pollution was the most serious. Research has revealed that Cd can cause renal and liver dysfunction in humans, and which is harmful to the human body even in the relatively small doses (Godt et al., 2006). For example, the 'Itai-Itai' disease that occurred in Toyama Prefecture, Japan, in the early 20th century is a manifestation of Cd poisoning.

There are many methods for remediating heavy metal pollution in soils, including physical and chemical remediation, bioremediation, and joint remediation. However, most of the methods are time-consuming and labor-intensive, and which is not suitable for the large-scale pollution remediation. Biochar can not only fix heavy metals in the soil, but also improve the soil's physicochemical properties (regulating soil pH and increasing soil pores), as well as provide nutrients (such as N, P, K) for the plant growth. In addition, biochar has a wide range of raw

materials and the materials are relatively inexpensive, suitable for large-scale production that is unmatched by other remediation methods. Biochar has made a great effect on Cd fixation in soil because of its structure, abundant pores and surface oxygen-containing functional groups (Li et al., 2016; Xu et al., 2016; Tan et al., 2017). The fixation mechanism of cadmium is roughly divided into four types, namely electrostatic attraction, complexation, cation exchange and precipitation (The fixation mechanism of biochar on soil cadmium is shown as Fig. 1). Among them, the immobilization by electrostatic attraction between molecules and ions is physical adsorption. There are complex mechanisms such as the agglomeration and sedimentation behaviour of biochar colloidal particles after the immobilisation of heavy metals in soil (Wang et al., 2013; Zhang et al., 2010). The fixation mechanisms of heavy metals by biochar are mostly based on the surface pore size and oxygen-containing functional groups (Table 1), while few researchers have explored the effect of surface charge in biochar on heavy metal fixation.

In this paper, the effect of the negative surface charge of biochar on soil Cd fixation is systematically studied, and the factors affecting the biochar surface charge are analysed; furthermore, the surface charge has been optimised to obtain a biochar with better Cd fixation properties.

* Corresponding author.

E-mail address: tanzx1977@163.com (Z. Tan).

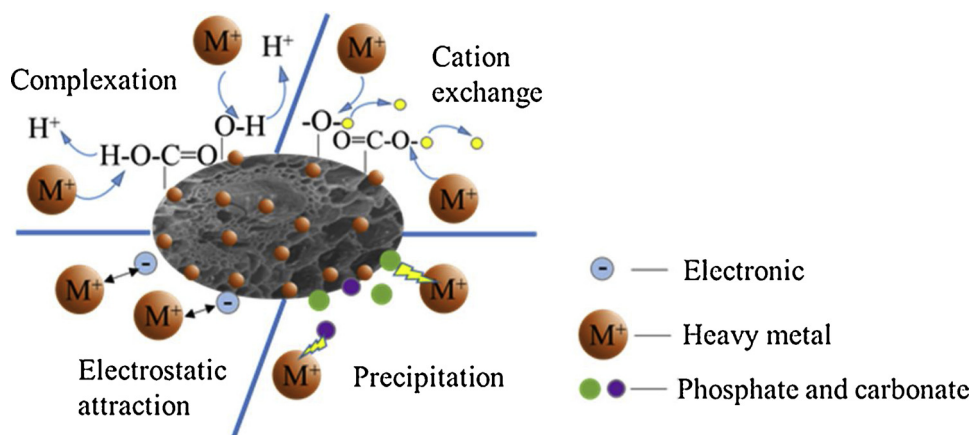


Fig. 1. The mechanism of biochar's fixation to cadmium.

Table 1

Factors affecting heavy metal fixation by biochar in the soil.

Biochar type	Contaminant	T (°C)	Effect factor on immobilisation	Reference
Oak wood	Cr	400–450	Sorption	Mohan et al., 2011
Hardwood	As	400	pH, dissolved organic carbon	Hartley et al., 2009
Sugar beet tailings	Cr	300	Electrostatic attraction, complexation	Dong et al., 2011
Crop straw	Cu	400	Surface complexation	Tong et al., 2011
Dairy manure	Pb	450	Hydroxypyromorphite, pH, organic C	Cao et al., 2011
Switch grass or corn cob	Cu, Cd, Ni, Zn	500	Inorganic fraction of biochar	Lima et al., 2010
Rice straw	Pb	300	Cation exchange capacity (CEC), non-electrostatic adsorption	Jiang et al., 2012
Dairy manure	Pb	200	Precipitation with phosphate	Cao and Harris, 2010
Sewage sludge	Pb	550	CEC, functional groups complexation, surface precipitation	Lu et al., 2012

2. Materials and methods

2.1. Biochar preparation

The rice straw was taken from the experimental field of Huazhong Agricultural University, Hubei Province, China, and naturally dried and stored for later use. The straw was crushed to the size of 3 cm and placed in the special pyrolysis furnace for thermal decomposition. During the heating process, the carrier gas is input from the bottom of the pyrolysis furnace to ensure anaerobic environment. The pyrolysis temperatures were set as 300, 400, 500, 600, and 700 °C respectively, the pyrolysis atmosphere was CO₂, gas flow rate was 40 L/h, the heating rate was set as 20 °C/min, and the residence time was 20 min. The carrier gas (CO₂) was pre-charged for 10 min to evacuate the air from the furnace. The biochar samples produced at 300, 400, 500, 600, and 700 °C in the CO₂ atmosphere are labelled C300, C400, C500, C600, and C700, respectively, and the original straw is labelled RS.

2.2. Characterisation of biochar

Determine Surface Zeta potential. First, 0.1 g biochar powder was placed in an erlenmeyer. Then, 200 mL of distilled water was added to it to make the suspension of 0.5 g/L, shaken at 150 rpm for 12 h. Finally, the Zeta potential analyser (British Malvern Instrument Co., Ltd. Britain) was used to measure the Zeta potential of the suspension (Sun, 2013). An elemental analyser (German element. Germany) was used to measure the C, H, O, and N contents in the biochar. A certain amount of biochar heated in the muffle furnace at 900 °C for 2 h to measure the ash content. The specific surface area was measured using a fully automatic specific surface area and pore size analyser (BET meter, AUTOSORB-1 MP-CR, USA) with method of N₂ adsorption-desorption (Guizani et al., 2014). The infrared spectra of the biochar samples were obtained using a Nicolet iS 50 Fourier-transform infrared spectrometer (FTIR). OMNIC 9 was used to control the data

collection. The scan range was 400–4000 cm⁻¹ with a resolution of 4.0 cm⁻¹ accumulated over 16 scans. The X-ray photoelectron spectra of the biochar samples were obtained by an XPS MULTILAB2000 (Thermo Fisher company. USA) at an energy resolution of 0.47 eV (Ag 3d5/2) and the minimum analysis area of 100 μm. The maps were fitted using AVANTAGE 4.75, where the standard peak for fitting to the sample C1s was set at 284.8 eV. Origin 8.6 was used to plot and analyze the data measured in the experiments.

2.3. Pot experiments and Cd measurement in plants

Wheat (Emai 596) was selected for pot experiments. The tested soil was topsoil collected from Shuanggang Village, Zhongfang Town, Linxiang City, Hunan Province, China. The type of soil is yellow-brown soil. The physicochemical property and Cd concentration of the soil are shown in Table 2.

In this experiment, the biochar was uniformly mixed with cadmium contaminated soil, apply the appropriate amount of deionized water in it, and then the wheat seeds were sown after one week of stabilization. The amount of sowing in each pot is the same, the mixed biochar is different. The cultivation of wheat seeds is purely to reflect the fixation effect of biochar on soil cadmium, so it is different from general phytoremediation. The soil and biochar were uniformly mixed in the pot, wherein the soil was 300 g and the biochar was 15 g. In addition, two control groups were added, one pot contained rice straw (RS) and soil, and the other is soil with the same weight (B). Twenty wheat seeds were

Table 2

Physicochemical properties and Cd content of the test soil.

pH	Avl. N mg/kg	Avl. P	Avl. K	Org. C g/kg	Tot. Cd mg/kg	CEC _T cmol/kg
5.5	147	18.27	173	42.5	12.848	68.45

Avl-Available; Org-Organic; Tot-Total; CEC_T-Total cation exchange capacity.

applied to each pot. During the growing period, the plants were watered (40 mL) with deionised water each day, the temperature was set to be 25 °C, the light conditions were 12 h light and 12 h dark alternately to ensure stable and normal plant growth. The plants were harvested after 30 days. In the harvest period, the wheat shoots were cut with scissors (at the junction of the root and shoot), and the underground part was discarded. The plant samples were washed with deionised water, and the gauze was used to blot away water attached to the plant surfaces. The plant height and fresh weight were measured. The plants were put in an oven at 115 °C for 0.5 h, dried at 75 °C for 24 h, and then measuring the dry weight of the plant.

The concentration of Cd in the plant samples was determined by microwave digestion and flame atomic absorption spectrometry (FAAS). Dried and chopped plant samples (0.3 g) were weighed on the analytical balance and poured into the digestion tank. To avoid the sample residue attaching to the tank wall, all samples were placed at the bottom of the digestion tank. Each sample was prepared in parallel three times, and a blank treatment was added as the control. The digestion tank was filled with pure nitric acid, shaken tightly, and put it for 1 h after tightening the piston. Then, the tank was placed into the microwave digestion instrument, and the program was set for plant digestion. After digestion and cooling, the sample (25 mL) was placed in fume cupboard and filtered to remove the scum. The Cd concentration of the sample was determined using FAAS.

3. Results and discussion

3.1. Effects of biochar surface charge on soil Cd uptake

Fig. 2(a) shows the zeta potential of the biochar prepared at different pyrolysis temperatures. As shown in Fig. 2(a), the surface potential of biochar is negative and exhibits certain negative electrical properties, and the amount of charge gradually decreases with the increasing pyrolysis temperature (-40.33 ~ -34.1 mV). Moreover, zeta potential of the biochar at 400 °C is -40.73 mV, which is lower than any other biochars, indicating that C400 has the largest number of negative surface charges on its surface. The above phenomenon is related to the deprotonation behavior of surface functional groups. The pH value of C300 (Fig. 3(b)) is 7.85, some functional groups on biochar's surface are not deprotonated. However, the pH of C400 is greater than 9 and the functional groups on the biochar's surface gradually deprotonate, so the negative charge generated by C400 is higher than C300. As the preparation temperature continues to rise (400–700 °C), all biochars have a pH greater than 9 (Fig. 3(b)), which has little effect on surface charge. But the number of oxygen-containing functional groups (-COH and -COOH) would decrease with increasing temperature, which reduces the deprotonation degree of oxygen-containing functional groups, resulting in the decrease of negative surface charge. Moreover, when the

biochar is pyrolysed at the high temperatures (≥ 600 °C), an increase in the aromatisation of the biochar occurs, resulting in the formation of π bonds, which can also form H-bonds with water, thus further neutralising surface negative charge.

It can be seen from Fig. 2(b) that the Cd concentration in the wheat cultivated by RS is higher than that of the blank control (B), indicating that there is no protective effect on Cd fixation after returning RS to the soil. The content of Cd in wheat treated with biochar produced at different pyrolysis all reduced significantly compared to the control samples (B and RS). The Cd concentration in the wheats treated by C300 is 2.56 mg/kg, higher than those of C400 (2.08 mg/kg), C500 (1.84 mg/kg), C600 (2.3 mg/kg) and C700 (1.31 mg/kg), respectively. That illustrated that biochars prepared under higher temperatures can fix more cadmium in soil and have the better protection effect on crops. Higher pyrolysis temperatures led to a decrease surface negative charge on biochar. There is some connection between the negative surface charge of the biochar and the fixation amount of Cd.

3.2. Effect of straw pyrolysis on the biochar surface charge

3.2.1. Effect of biochar ash and pH on zeta potential

Fig. 3 shows the ash contents of the biochar samples, as well as the pH values of the biochar suspensions. Previous studies have shown that the pyrolysis temperature has a great influence on the physicochemical properties of biochar (Chen et al., 2016; Cantrell et al., 2012). It can be seen from Fig. 3 that the ash content of the biochar increases from 29.92% to 44.09% with the increasing temperature from 300 to 700 °C, as well as the pH value increases from 7.85 to 9.81. The increase in ash content is mainly due to the increase in the amount of alkali metal during pyrolysis. Studies have shown that the ash, which comprises SiO₂, Al₂O₃, CaO, and various phosphates and carbonates, is responsible for the changes in the biochar alkalinity (Novak et al., 2009; Yuan et al., 2011). During the biochar preparation, elements such as Ca, P, and Mg in the biomass are left in solid production to form alkaline substances such as calcium carbonate and phosphate. The increase in pH of the biochar mainly comes from these mineral salts (Boehm, 1994; Yuan et al., 2011). When biochar is added into the deionized water (pH = 7 of deionized water), these alkaline substances are dissolved in water to raise the pH.

Add acid or alkaline in biochar, make the suspension pH to 2, 3, 4, 5, 6, 7, 8, 9, 10, 11, 12, respectively. And then measure biochar's zeta potential, the zeta potential at different pH values is shown in Fig. 4. As can be seen from Fig. 4, with the increase of pH, zeta potential of biochar showed a downward trend, which was the same as the conclusion reported by Zhang and Yu (Zhang et al., 2016; Yu et al., 2018). This phenomenon is due to the different degree of protonation of hydroxyl and carboxyl groups at different pH values. Alkaline conditions increase the deprotonation degree of oxygen-containing functional

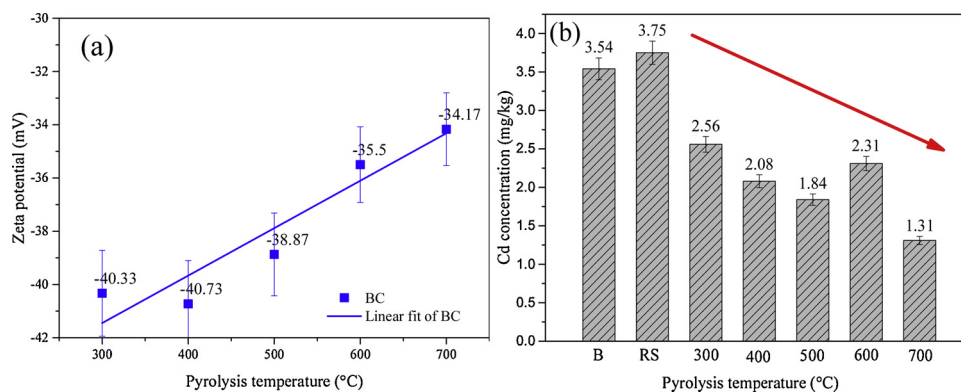


Fig. 2. Zeta potential of the biochar and Cd content of the wheat shoots. B-no added group; RS-added straw group.

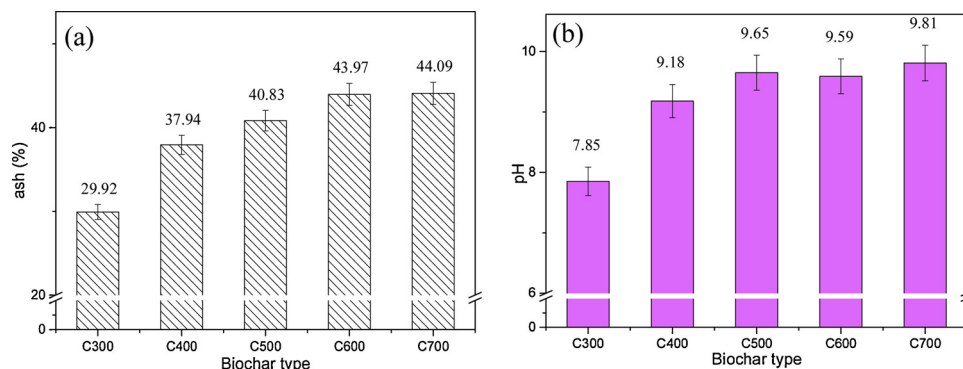


Fig. 3. Ash content and pH value of the biochar samples. a-Ash content of the biochar; b-pH value of the biochar.

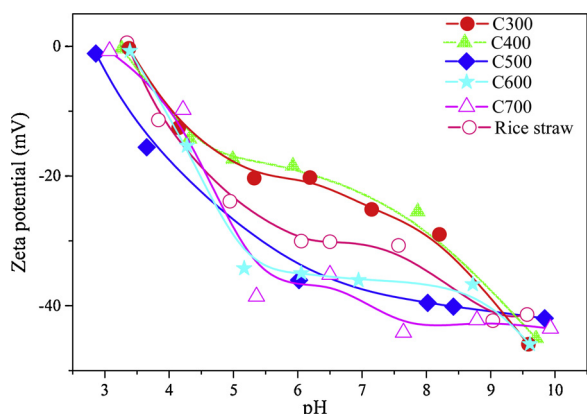


Fig. 4. Zeta potential of biochar at different pH values.

groups, resulting in a decrease in zeta potential. The pH at the time when the zeta potential is zero is the pH_{IEP} . After the pyrolysis of biochar, its isoelectric point (pH_{IEP}) is between 2 and 5 (Fang et al., 2013; Teixido et al., 2011; Lu et al., 2013), and the pH of the biochar suspension in this experiment is higher than 7 ($> pH_{IEP}$). Thus, the surface of the biochar particles is negatively charged, and the same conclusion has been drawn from Gao (Gao et al., 2018). Under different preparation conditions, biochar can have a different quantity of negative

surface charge.

Fig. 5 shows the mechanism of the effect of ash and pH on the surface charge of biochar. The ash contents of the biochar samples prepared at distinct temperatures are different, which leads to the change of pH value of biochar and further affect the deprotonation of oxygen-containing functional groups on the biochar surface.

3.2.2. Effects of oxygen-containing functional groups (OCFGs) on the surface negative charge

Fig. 6 shows the infrared spectra of the biochar samples prepared at different pyrolysis temperatures. The hydroxyl band is present at 3420 cm^{-1} . A broad and strong absorption peak appears in the $3400\text{--}3200\text{ cm}^{-1}$ region. With the increasing pyrolysis temperature, the absorption peak of -OH gradually shifted to the lower wavenumbers from 3419.4 cm^{-1} (RS) to 3412.46 cm^{-1} (C300), 3412.32 cm^{-1} (C400), 3394.29 cm^{-1} (C500), 3385.50 cm^{-1} (C600) and 3418.37 cm^{-1} (C700). This change in wavenumber is due to an increase number of unsaturated groups around the hydroxyl group. This phenomenon reflects the conversion of the carbon skeleton of biochar from a basic saturated hydrocarbon chain to an unsaturated aromatic structure, which in turn leads to a decrease in the content of various oxygen groups. Carbonyl vibrations were observed at $1750\text{--}1600\text{ cm}^{-1}$, and this is a characteristic peak of carboxylic acids. Because of the presence of H-bonds, carboxylic acids usually exist in dimeric form, in which the OH stretching frequency is quite low. A broad and scattered

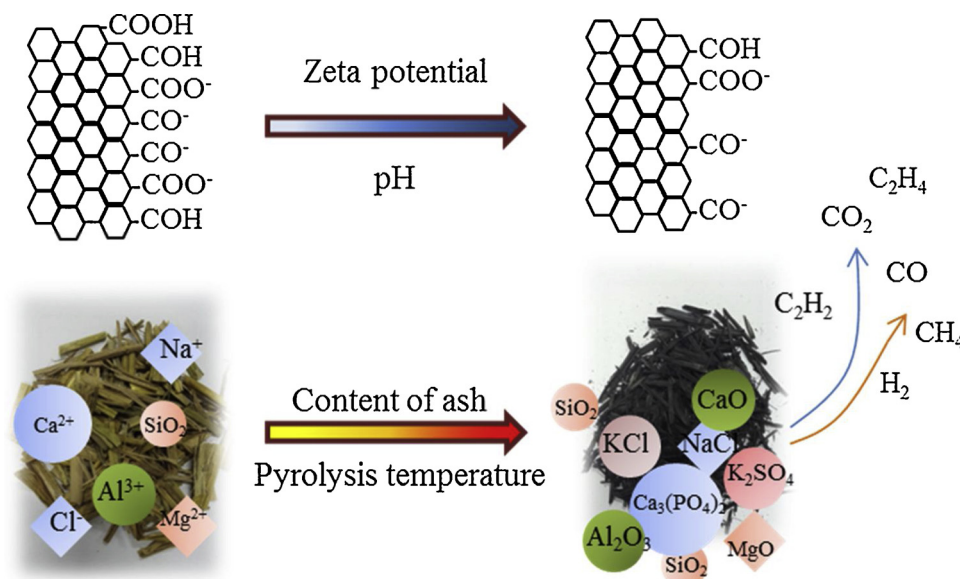


Fig. 5. Effect of ash and pH on the negative surface charge.

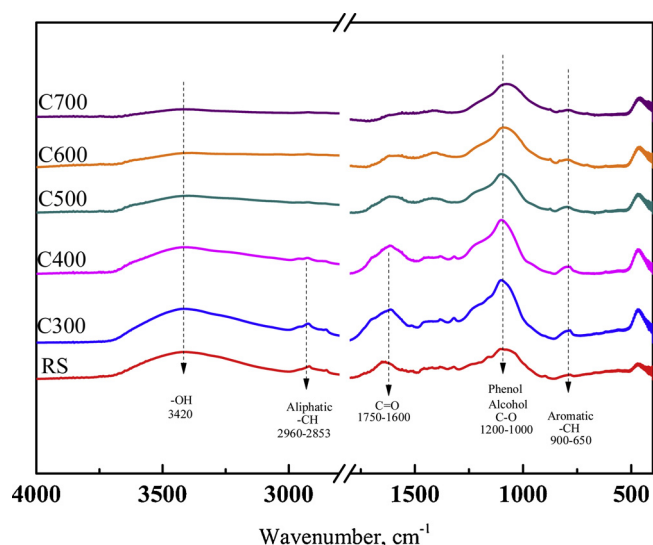
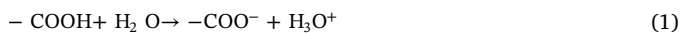


Fig. 6. Infrared spectra of the biochar samples.

peak is observed in the 3200–2500 cm^{-1} , which is also a characteristic peak of carboxylic acids. The 1200–1000 cm^{-1} region is characteristic peak of the C–O bond vibrations of alcohols and phenols. The vibrational intensity of these bands decreases with the increasing pyrolysis temperature, which indicates that the content of alcohol and phenol is reduced. In addition, as the pyrolysis temperature rises, the intensity of the aromatic C–H peaks at 900–650 cm^{-1} gradually increase, illustrating that the aromatic structure is enhanced.

The XPS results were analysed to identify the effect of the OCFGs content on the surface negative charge of the biochar, as shown in Fig. 7. The relative content of OCFGs was obtained by fitting to the XPS plots (shown as Fig. 8). As shown in Fig. 7, as the pyrolysis temperature increases from 300 to 700 $^{\circ}\text{C}$, the C–C/C–H content gradually increases from 56.95% to 68.52%, which is due to the increased degree of carbonization and aromatization of biochars. The increase in carbonisation is also the main reason for increasing specific surface area and the porosity of biochar. The alcohol and phenol hydroxy groups reduced from 25.97% (C300) to 25.5% (C400), 24.46% (C500), 23.45% (C600), and 16.64% (C700). The total amount of oxygen-containing functional groups decreased with the increase of preparation temperature. Among these oxygen-containing functional groups, hydroxyl and carboxylic acid groups become negatively charged on deprotonation (Formula 1 and 2):



As shown in Fig. 8, with the increasing pyrolysis temperature, the total content of $-\text{COH}$ and COOH decreases from 30.77% (C300) to 19.74% (C700); this trend is consistent with the change of zeta potential shown in Fig. 2(a); that is, the surface negative charge decreases with the increasing pyrolysis temperature. It is indicated that these two functional groups play a decisive role in the surface negative charge of the biochar. The hydroxyl content is much higher than the carboxyl, so hydroxyl has a greater influence on the surface negative charge. Fig. 9 shows the relationship between the oxygen content and the surface negative charge of the biochar. As shown in the figure, the content of oxygen-containing functional groups (the total amount of hydroxyl and carboxyl groups) gradually decreases with the increasing pyrolysis temperature, resulting in a reduction in the number of deprotonatable groups and a corresponding drop in the surface negative charge.

3.2.3. Effect of the polarity of the biochar on the surface negative charge

Table 3 shows the basic elemental contents and atomic ratio of the

biochar samples at different pyrolysis temperatures. $(\text{O} + \text{N})/\text{C}$ is the polarity index, and larger values indicate greater polarity (Chen et al., 2005). The O/C and $(\text{O} + \text{N})/\text{C}$ values in the biochar show an initial decreasing trend, which then increases with the increasing pyrolysis temperature, and the inflection point is found at the C600 sample. The reason for the high O/C and $(\text{O} + \text{N})/\text{C}$ values in C700 may be the presence of coke on the biochar surface, which undergoes additional cracking reactions (Formula 3) with CO_2 at high temperatures (≥ 600 $^{\circ}\text{C}$) resulting in lower carbon content.



On one hand, the polarity characterises the hydrophilicity; on the other hand, polar molecules exhibit a certain charge, and the surface charge is partly determined by the polarity of the biochar. When bonded atoms have different electronegativities, the charge distribution of the covalent bonds is uneven. Thus, the electrons are pulled toward the different atoms to different degrees, resulting in bond polarisation. Fig. 10 shows how the polarisation affects the surface charge of the biochar. In the carbon skeleton of biochar, when atoms such as O and N combine with C and H, the electrons are distributed toward the more electronegative O and N atoms. This electronic shift causes the biochar surface to carry the negative charge; thus, the greater the polarisation of the biochar, the stronger is the surface negative charge. However, polarisation is only a secondary factor affecting the surface charge and is not the main factor. Instead, the surface negative charge of the biochar is significantly affected by the content of oxygen-containing functional groups.

3.2.4. Effect of H-bonds in the biochar on surface negative charge

When the covalent molecule (X–H) containing hydrogen atom is close to another electronegative atom (Y), a special intermolecular or intramolecular interaction formed between hydrogen and Y atoms is called hydrogen bonding (X–H \cdots Y). The zeta potential of the biochar is determined using a suspension of solid particles, and the different functional groups exposed at the surface of the biochar can form H-bonds with water molecules, which can affect the zeta potential of the biochar surface and further effect the surface charge. Fig. 11 shows a schematic of the H-bonding between different functional groups and water molecules in the biochar suspension. The oxygen in the hydroxyl, carboxyl, carbonyl as well as the nitrogen atoms in amino functional groups can form H-bonds with hydrogen atoms in H_2O , and the oxygen atoms in H_2O also can generate H-bonds with the hydrogen atoms of the hydroxyl groups. The generation of H-bonds will neutralise some of the surface charge generated by bond polarisation, which reduces the surface negative charge of the biochar. As shown in Table 3, the polarity index of the biochar decreases initially and then increases, indicating that the negative charge induced by bond polarisation at the biochar surface decreases at first and then increases with the increasing pyrolysis temperature. When the biochar is pyrolysed at the high temperatures (≥ 600 $^{\circ}\text{C}$), an increase in the aromatisation of the biochar occurs, resulting in the formation of π bonds, which can also form H-bonds with water (Harvey et al., 2011), thus further neutralising surface charge produced by polarisation. Consequently, the surface negative charge is significantly weakened. The increase in the degree of aromatisation of biochar reduces the number of oxygen-containing functional groups in the biochar, which also leads to a reduction in the number of negatively charged sites and a decrease in the surface negative charge.

3.3. Conditions for the optimal biochar preparation for fixing Cd from soil

The physical and chemical properties of biochar have a great influence on the in-situ fixation of Cd in soil and crop protection. The negative charge on biochar surface is negatively correlated with the fixation effect, i.e. the less negative charge on the surface of the biochar, the greater the fixation effect of Cd. Fig. 12 shows the factors

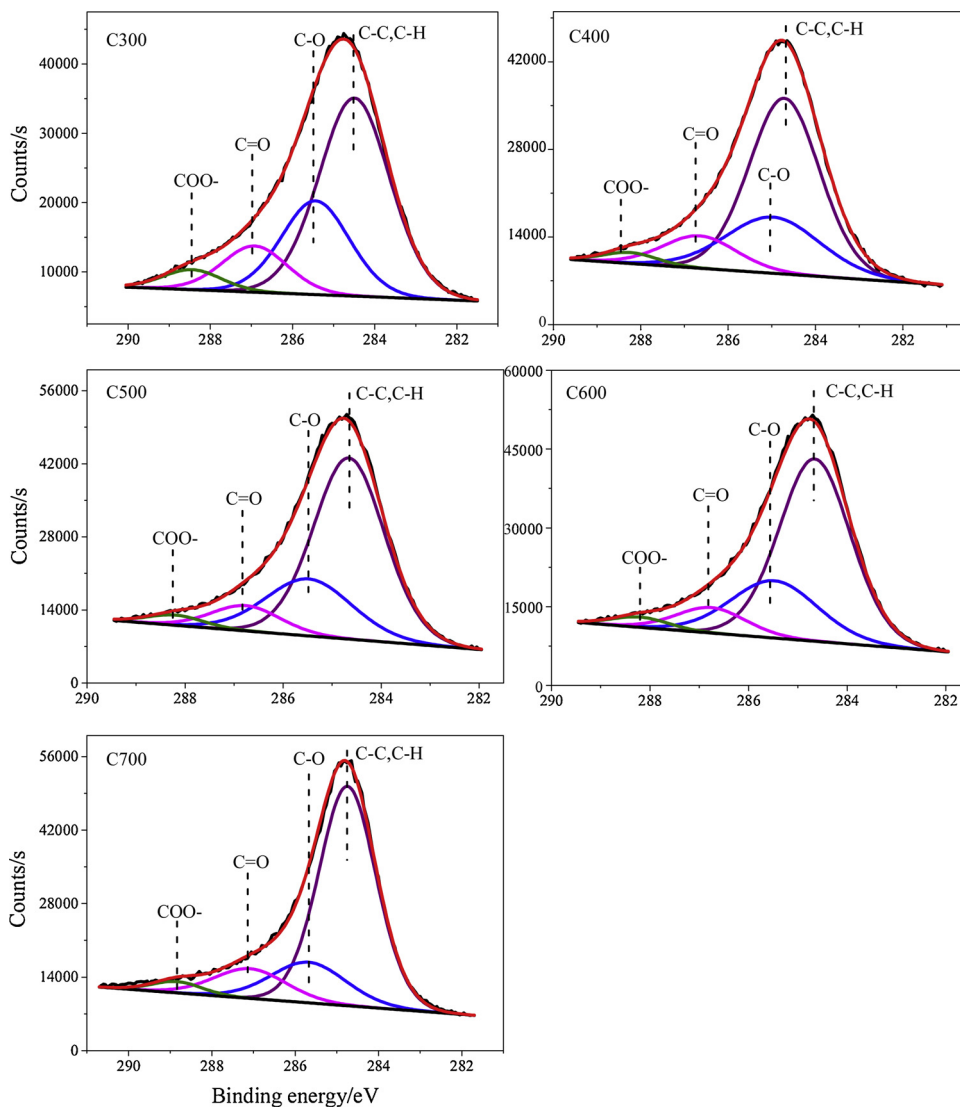


Fig. 7. XPS spectra of the biochar samples.

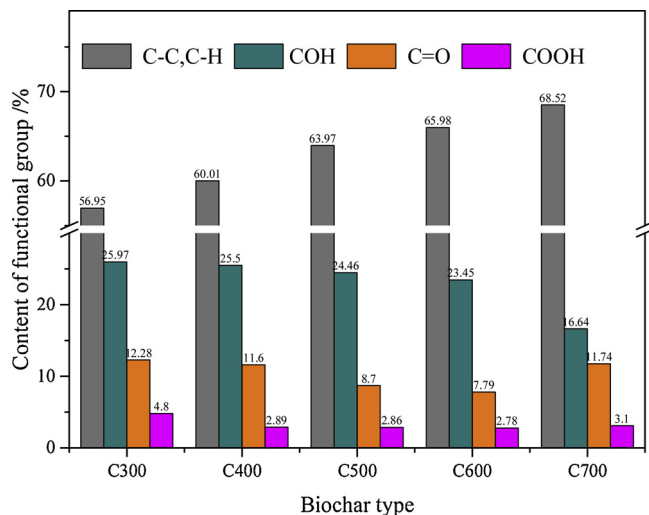


Fig. 8. The relative content of OCFGs in biochar.

influencing the biochar surface charge: the OCFG content, ash, pH, polarity, and H-bonds. The first three factors have the positive impact on the negative charge on biochar's surface; that is to say, the increasing contents of -COH and -COOH groups (or an increase in pH and polarity) increase the negative charge of biochar. In contrast, H-bonds have the opposite effect on negative charge; that is, an increase in the number of H-bonds reduces the surface charge on biochar's surface. Among the four influencing factors, the amount of OCFG has the greatest influence on the negative charge, especially the content of -COH.

From the colloid stability, the repulsive force between colloidal particles will increase with the increase of absolute zeta potential on the colloidal surface, resulting in the more stable the dispersed colloidal particles are, and it is not easy to agglomerate and precipitate. After the biochar is applied to the soil, it forms the mixed colloid with the soil clay, which causes the zeta potential of the mixed colloid to change to varying degrees, and further affecting the stability of the mixed colloid. The absolute value of zeta potential of biochar decreases gradually with the increase of pyrolysis temperature, which leads to the decrease of biochar colloid stability. Biochar is more likely to coagulate with cadmium, resulting in a decrease in the effective cadmium content of plants. The better the fixation effect of cadmium by biochar, the stronger the protection of plants is.

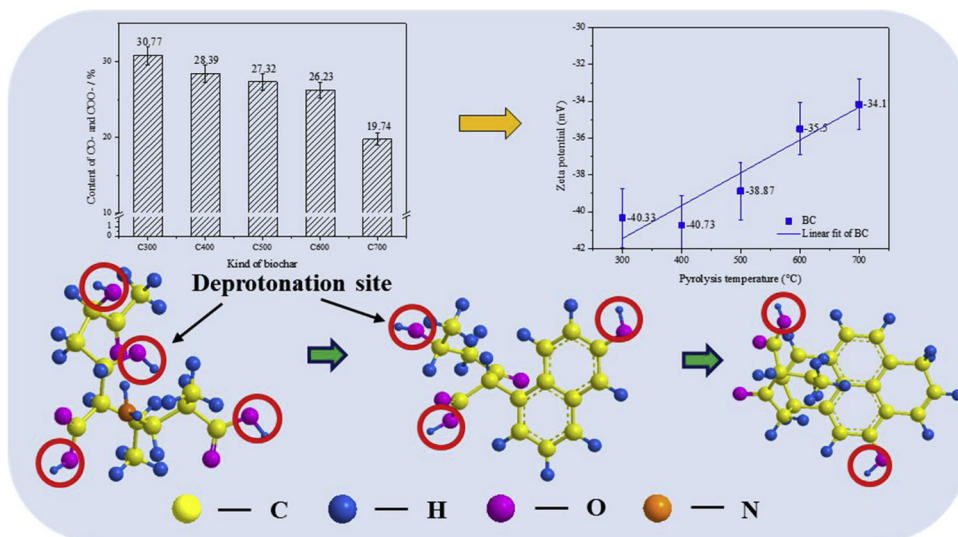


Fig. 9. Relationship between the oxygen content and the surface negative charge of the biochar.

Table 3
Elemental contents and atomic ratios of the biochar samples.

Biochar	Yield (%)	SA (m ² /g)	C (%)	H (%)	O (%)	N (%)	H/C	O/C	(O + N)/C
RS	-	2.53	32.08	5.33	35.32	1.06	1.99	0.83	0.85
C300	57.04	4.54	35.96	4.64	20.26	1.08	1.55	0.42	0.45
C400	44.36	9.52	37.07	3.13	15.49	0.96	1.01	0.31	0.34
C500	40.92	15.27	37.23	2.21	14.53	0.86	0.71	0.29	0.31
C600	39.88	11.16	40.91	1.08	12.70	0.87	0.32	0.23	0.25
C700	37.7	60.12	38.43	0.62	12.97	0.80	0.19	0.25	0.27

The negative charge on the biochar’s surface can be adjusted by setting the preparation conditions to obtain the best biochar for fixing Cd in the soil. According to the above analysis, the Cd content absorbed by plants cultivated by C700 is the lowest. In the next study, we conducted a pot experiment used the biochar prepared at the pyrolysis temperature of 400, 600 and 800 °C (C400, C600 and C800) in order to determine the effect of pyrolysis temperature on soil Cd fixation. In addition, the basic properties of biochar were also determined such as the zeta potential, pH, ash, polarity, and functional groups.

Fig. 13 shows the zeta potential of the biochar suspension after high-temperature optimisation. As the pyrolysis temperature rose from 400 to 800 °C, the zeta potential rose from -40.73 to -35.5 to -23.5 mV for C400, C600, and C800, respectively, which is consistent with the aforementioned reduction in the surface negative charge.

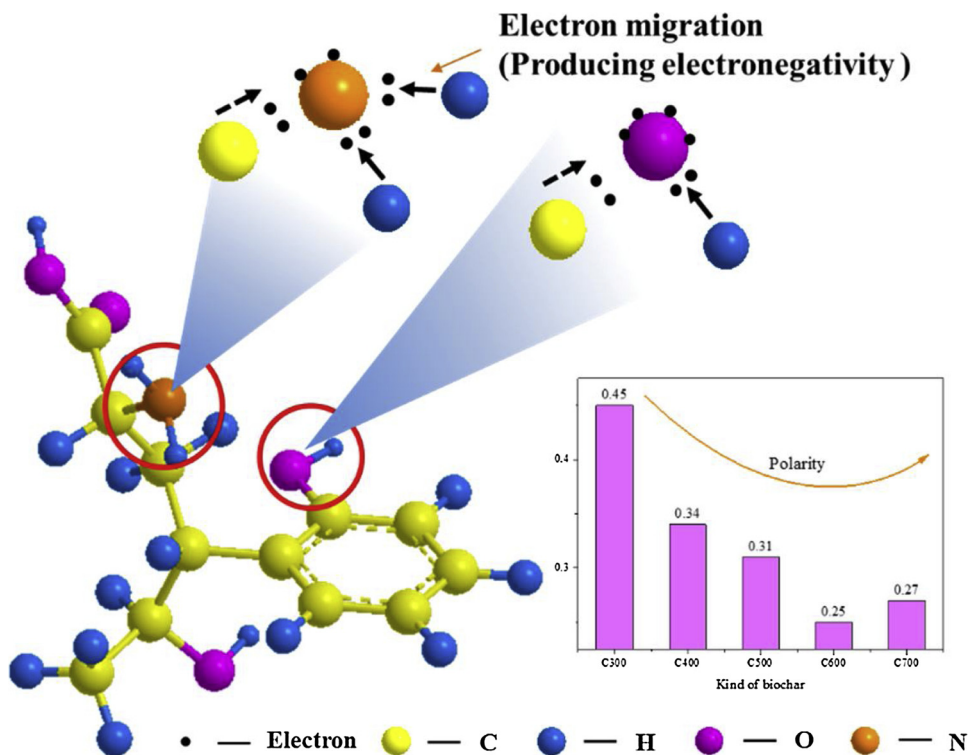


Fig. 10. Mechanism of the influence of polarisation on the surface negative charge.

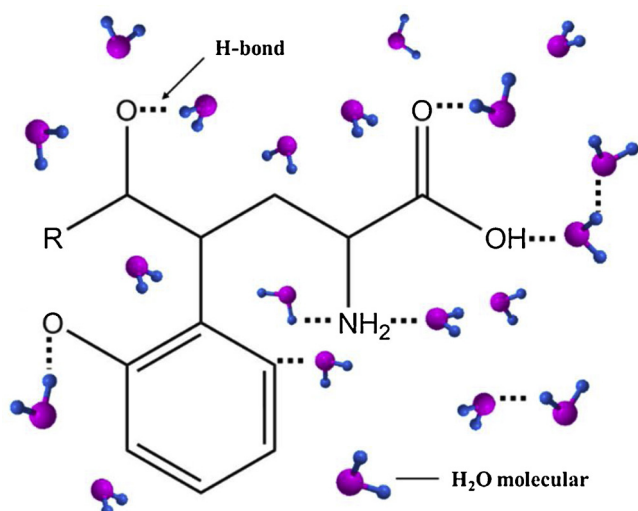


Fig. 11. H-bonds between different functional groups and water molecules in an aqueous suspension of biochar.

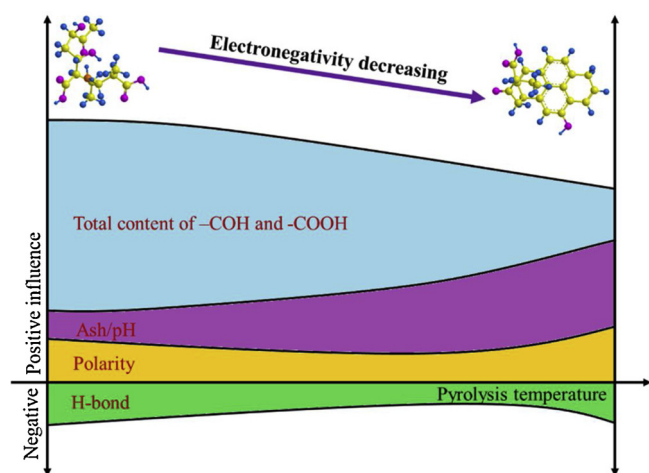


Fig. 12. Factors influencing the biochar surface negative charge.

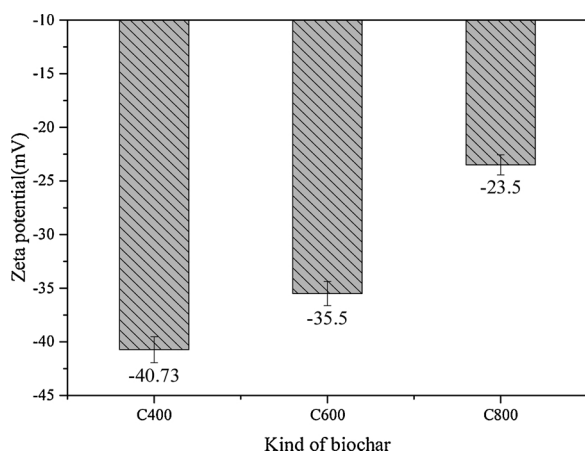


Fig. 13. Zeta potential of the biochar after high-temperature optimisation.

Next, we discuss the effects of the biochar properties on the surface negative charge.

3.3.1. pH and ash

Fig. 14 shows the pH and ash contents of the biochar samples

prepared at three pyrolysis temperatures. It can be seen from Fig. 14 that the pH increased from 9.18 (C400) to 9.83 (C800) with the increasing pyrolysis temperature as well as the ash content increased from 37.94% (C400) to 49.87% (C800). The increase of ash content leads to the increase of pH value, dephosphorization degree and surface negative charge. However, the increase of ash content also reflects the decrease of functional group content.

3.3.2. Hydroxyl and carboxylic acid groups

Fig. 15 illustrates the content of $-\text{COH}$ and $-\text{COOH}$ on the biochar' surfaces prepared at different pyrolysis temperatures, as determined by XPS. The total content of $-\text{COH}$ and $-\text{COOH}$ decreases from 28.39% (C400) to 14.3% (C800), as well as the content of hydroxyl groups is significantly reduced from 25.5% (C400) to 9.79% (C800). These two functional groups have a significant influence on the surface negative charge of the biochar, the impact of COH is even greater.

3.3.3. Polarity index and H-bonds

Fig. 16 shows the polarity indexes $(\text{O} + \text{N})/\text{C}$ of the biochar samples prepared at different pyrolysis temperatures. With increasing pyrolysis temperature, the polarity index of the biochar decreases at first and then increases. The biochar produced below 600°C has a high polarity index, resulting in negative charge at the biochar's surface. When the pyrolysis temperature is higher than 600°C , the content of functional group and the hydrogen bond in biochar decreases, while the aromaticity increases. The effects of polar groups and hydrogen bonds on negative charges in biochars are interactional. In soil colloids, the formation of H-bonds neutralises a part of the negative charge generated by the polar groups, which weakens the negative charge of the biochar's surface. The neutralisation of these two effects is one of the reasons for the reduction in the biochar surface negative charge.

3.4. Verification of Cd fixation using biochar with optimised surface charge in contaminated soil

Fig. 17 shows the concentration and removal rate of Cd in the treated groups compared to that in the control group. The results show that the biochar prepared at high temperature had a better protective effect (i.e. more Cd fixation) than biochar prepared at lower temperatures. As shown in the figure, the Cd concentrations in wheat shoots cultivated with biochar are significantly lower than that of the blank group (B). The Cd concentration in plants decreases with the increasing pyrolysis temperature, from 3.54 to 2.08, 2.3, and 0.88 mg/kg for B, C400, C600, and C800, respectively. The reduction of Cd in plant indicated the reduced availability of Cd for uptake by crops after the addition of biochar, and the percentage of Cd reduction in wheat treated with C400, C600, and C800 are 41.24%, 35.03% and 75.14%, indicating that C800 has the best protective effect for crops.

Based on the charge changes in the biochar surface shown in Fig. 13 and the change of Cd concentration in wheat shoots shown in Fig. 17 can be concluded that the use of biochar with a lower surface charge can reduce the Cd concentration in wheat significantly. From the stability of the colloid, the larger the absolute value of zeta potential on colloid, the greater the repulsive force between the colloidal particles, the more stable the dispersed colloidal particles, and the less likely to agglomerate and precipitate. As the increasing pyrolysis temperature, the absolute value of the zeta potential of biochar gradually decreases, resulting in a decrease in the stability of biochar colloid. The biochar colloid adsorbing heavy metal cadmium is agglomerated and settled, resulting in a decrease in the effective heavy metal cadmium, the cadmium content in the plant is reduced. The optimised biochar (prepared at 800°C , which has a lower negative charge) had a better protective effect on wheat, which is consistent with the above conjecture. Therefore, the optimal biochar preparation temperature for soil Cd fixation is 800°C .

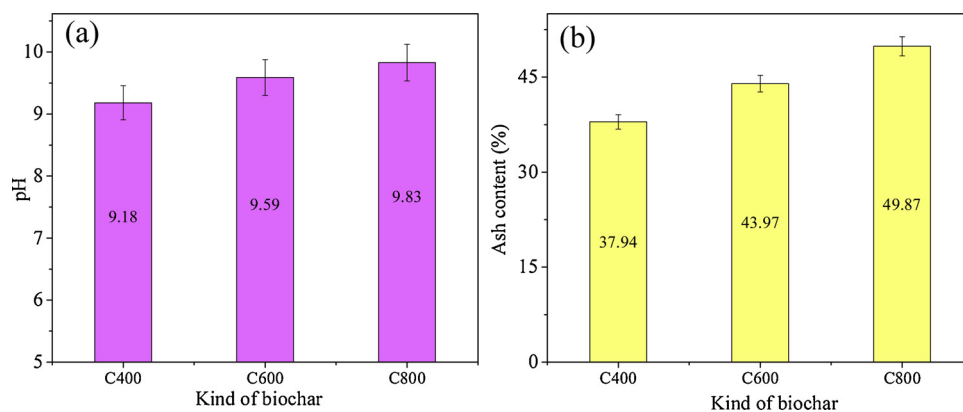


Fig. 14. pH and ash content of biochar.

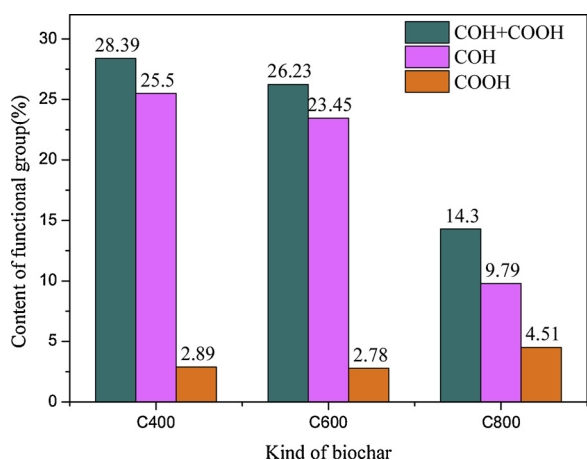


Fig. 15. The contents of -COH and -COOH in the biochar samples.

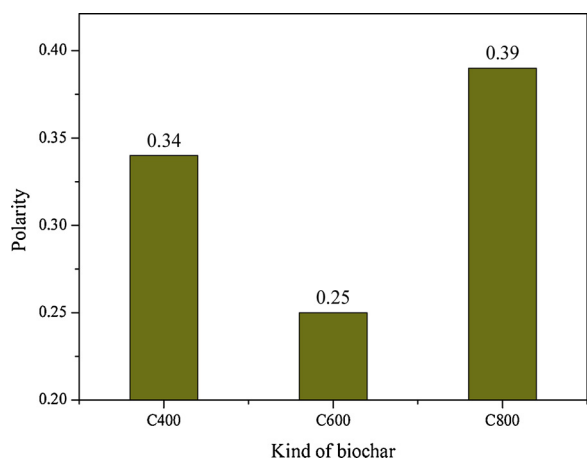


Fig. 16. Polarity indexes of biochar samples prepared at different pyrolysis temperatures.

4. Conclusion

The negative charge on biochar's surface has an effect on the fixation of soil Cd. A less negative surface charge results in a better protective effect for crops after the addition of the biochar to the soil. The surface charge of the biochar is affected by the pyrolysis temperature, which results in changes to various biochar properties.

The factors affecting the surface charge of biochar are the pH, ash, oxygen-containing functional groups, polarity, and H-bonds. The first three can increase the surface negative charge, whereas the H-bonds

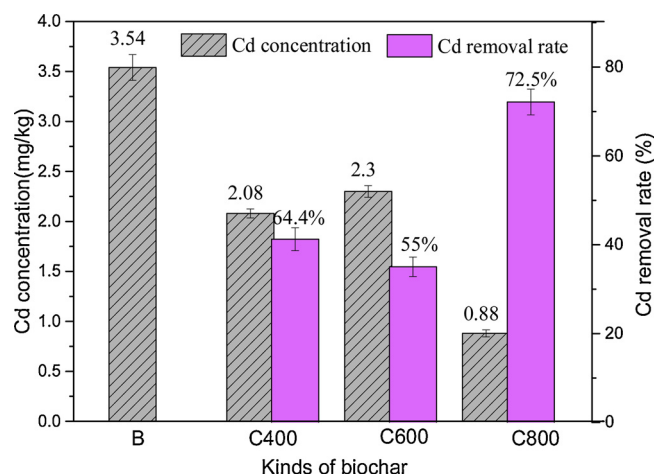


Fig. 17. the concentration and removal rate of Cd in the treated groups compared to that in the control group.

reduce it. The most important factor affecting the surface negative charge of the biochar is the number of oxygen-containing functional groups, i.e. the negatively charged sites of the biochar are the -OH and -COOH, and hydroxyl is the most important functional group. As the pyrolysis temperature increases, the large reduction in the number of hydroxyl groups results in a significant loss of surface negative charge.

The pyrolysis of biochar was optimised at the high temperature (800 °C), resulting in the changes of several physicochemical properties (pH, ash, oxygen-containing functional groups, and polar groups) in biochar and reducing the negative surface charge. Pot experiments show that the use of the high-temperature biochar in soil prevented the uptake of Cd by wheat plants, suggesting that biochar with a low surface charge prepared at 800 °C is optimal for the fixation of Cd in soil.

Acknowledgements

This study was supported by the National Natural Science Foundation of China (No.41571283), the National Key Research and Development Program of China (2018YFD0800703, 2016YFD0800702) and the Fundamental Research Funds for the Central Universities (2662018PY078).

References

Boehm, H.P., 1994. Some aspects of the surface chemistry of carbon blacks and other carbons. *Carbon* 32 (5), 759-769.
 Cantrell, K.B., Hunt, P.G., Uchimiya, M., Novak, J.M., Ro, K.S., 2012. Impact of pyrolysis temperature and manure source on physicochemical characteristics of biochar. *Bioresour. Technol.* 107, 419-428.

- Cao, X., Harris, W., 2010. Properties of dairy-manure-derived biochar pertinent to its potential use in remediation. *Bioresour. Technol.* 101 (14), 5222–5228.
- Cao, X., Ma, L., Liang, Y., Gao, B., Harris, W., 2011. Simultaneous immobilization of lead and atrazine in contaminated soils using dairy-manure biochar. *Environ. Sci. Technol.* 45 (11), 4884–4889.
- Chen, B., Johnson, E.J., Chefetz, B., Zhu, L., Xing, B., 2005. Sorption of polar and non-polar aromatic organic contaminants by plant cuticular materials: role of polarity and accessibility. *Environ. Sci. Technol.* 39 (16), 6138–6146.
- Chen, Z., Chen, B., Chiou, C.T., 2016. Fast and slow rates of naphthalene sorption to biochars produced at different temperatures. *Environ. Sci. Technol.* 46 (20), 11104–11111.
- Dong, X., Ma, L.Q., Li, Y., 2011. Characteristics and mechanisms of hexavalent chromium removal by biochar from sugar beet tailing. *J. Hazard. Mater.* 190 (1-3), 909–915.
- Fang, Q.L., Chen, B.L., Lin, Y.J., Guan, Y.T., 2013. Aromatic and hydrophobic surfaces of wood-derived biochar enhance perchlorate adsorption via hydrogen bonding to oxygen containing organic groups. *Environment Sci. Technology* 48, 279–288.
- Gao, L.Y., Deng, J.H., Tang, G.Q., Cai, K.Z., Cai, Y.X., 2018. Adsorption characteristics and mechanism of Cd^{2+} by eucalyptus leaf biochar at different temperatures. *China Environ. Sci.* 3, 1001–1009 (in Chinese).
- Godt, J., Scheidig, F., Grosse-Siustrup, C., Esche, V., Brandenburg, P., Reich, A., et al., 2006. The toxicity of cadmium and resulting hazards for human health. *J. Occup. Med. Toxicol.* 1 (1), 22.
- Guizani, C., Escudero Sanz, F.J., Salvador, S., 2014. Effects of CO_2 on biomass fast pyrolysis: reaction rate, gas yields and char reactive properties. *Fuel* 116, 310–320.
- Hartley, W., Dickinson, N.M., Riby, P., Lepp, N.W., 2009. Arsenic mobility in brownfield soils amended with green waste compost or biochar and planted with miscanthus. *Environ. Pollut.* 157 (10), 2654–2662.
- Harvey, O.R., Herbert, B.E., Rhue, R.D., Kuo, L.J., 2011. Metal interactions at the biochar-water interface: energetics and structure-sorption relationships elucidated by flow adsorption microcalorimetry. *Environ. Sci. Technol.* 45 (13), 5550.
- Jiang, T.Y., Jiang, J., Xu, R.K., Li, Z., 2012. Adsorption of Pb (II) on variable charge soils amended with rice-straw derived biochar. *Chemosphere* 89 (3), 249–256.
- Li, Z., Qi, X., Fan, X., Du, Z., Hu, C., Zhao, Z., et al., 2016. Amending the seedling bed of eggplant with biochar can further immobilize Cd in contaminated soils. *Sci. Total Environ.* 572, 626–633.
- Lima, I.M., Boateng, A.A., Klasson, K.T., 2010. Physicochemical and adsorptive properties of fast-pyrolysis bio-chars and their steam activated counterparts. *J. Chem. Technol. Biotechnol.* 85 (11), 1515–1521.
- Lu, H., Zhang, W., Wang, S., Zhuang, L., Yang, Y., Qiu, R., 2013. Characterization of sewage sludge-derived biochars from different feedstocks and pyrolysis temperatures. *J. Anal. Appl. Pyrolysis* 102, 137–143.
- Lu, H., Zhang, W., Yang, Y., Huang, X., Wang, S., Qiu, R., 2012. Relative distribution of Pb^{2+} sorption mechanisms by sludge-derived biochar. *Water Res.* 46 (3), 854–862.
- Mohan, D., Rajput, S., Singh, V.K., Steele, P.H., Pittman, C.U., 2011. Modeling and evaluation of chromium remediation from water using low cost bio-char, a green adsorbent. *J. Hazard. Mater.* 188 (1-3), 319–333.
- Novak, J.M., Busscher, W.J., Laird, D.L., Ahmedna, M., Watts, D.W., Niandou, M.A.S., 2009. Impact of biochar amendment on fertility of a southeastern coastal plain soil. *Soil Sci. Soc. J.* 174 (2), 105–112.
- Sun, H.W., 2013. *Biochar and Environment*. Chemical Industry Press, Beijing (in Chinese).
- Tan, Z., Wang, Y., Kasiulienė, Alfreida, Huang, C., Ai, P., 2017. Cadmium removal potential by rice straw-derived magnetic biochar. *Clean Technol. Environ. Policy* 19 (3), 761–774.
- Teixido, M., Pignatello, J.J., Beltran, J.L., Granados, M., Peccia, J., 2011. Speciation of the ionizable antibiotic sulfamethazine on black carbon (biochar). *Environ. Sci. Technol.* 45 (23), 10020–10027.
- Tong, X.J., Li, J.Y., Yuan, J.H., Xu, R.K., 2011. Adsorption of Cu (II) by biochars generated from three crop straws. *Chem. Eng. J.* 172 (2-3), 828–834.
- Toth, G., Hermann, T., da Silva, M.R., Montanarella, L., 2016. Heavy metals in agricultural soils of the European Union with implications for food safety. *Environ. Int.* 88, 299–309.
- Wang, D., Zhang, W., Hao, X., Zhou, D., 2013. Transport of biochar particles in saturated granular media: effects of pyrolysis temperature and particle size. *Environ. Sci. Technol.* 47 (2), 821–828.
- Xu, P., Sun, C.X., Ye, X.Z., Xiao, W.D., Zhang, Q., Wang, Q., 2016. The effect of biochar and crop straws on heavy metal bioavailability and plant accumulation in a Cd and Pb polluted soil. *Ecotoxicol. Environ. Saf.* 132, 94–100.
- Yu, J.G., Zhang, X.W., Wang, D., Tang, Q., Li, P., 2018. Preparation, characterization and adsorption properties of hydrothermal modified biochar. *Industrial Water Treatment* 9, 53–57 (in Chinese).
- Yuan, J.H., Xu, R.K., Zhang, H., 2011. The forms of alkalis in the biochar produced from crop residues at different temperatures. *Bioresour. Technol.* 102 (3), 3488–3497.
- Zhang, M.Y., Li, F.M., Lu, L., Gu, S.R., 2016. Adsorption characteristics of methylene blue by reed biochar. *J. Chinese Marine University: Natural Sci. Edition.* 12, 96–103 (in Chinese).
- Zhang, W., Niu, J., Morales, Verónica L., Chen, X., Hay, A.G., Lehmann, J., et al., 2010. Transport and retention of biochar particles in porous media: effect of Ph, ionic strength, and particle size. *Ecohydrology* 3 (4), 497–508.